Synthesis and thermal stability of cubic ZnO in the salt nanocomposites

P. S. Sokolov,[a,b] A. N. Baranov,[c] Zh. V. Dobrokhotova,[d] and V. L. Solozhenko[a]*

[a]*Laboratory of Mechanical and Thermodynamic Properties of Materials, LPMTM-CNRS, Université Paris 13, 99 avenue J. B. Clément, 93430 Villetaneuse, France. E-mail: vladimir.solozhenko@univ-paris13.fr*
[b]*Department of Materials Science, M. V. Lomonosov Moscow State University, 1 Leninskie gory, 119991 Moscow, Russian Federation. E-mail: sokolov@inorg.chem.msu.ru*
[c]*Department of Chemistry, M. V. Lomonosov Moscow State University, 1 Leninskie gory, 119991 Moscow, Russian Federation. Fax: +7 (495) 939 0998. E-mail: anb@inorg.chem.msu.ru*
[d]*N. S. Kurnakov Institute of General and Inorganic Chemistry, Russian Academy of Sciences, 31 Leninsky prosp., 119991 Moscow, Russian Federation*

Cubic zinc oxide (rs-ZnO), metastable under normal conditions, was synthesized from the wurtzite modification (w-ZnO) at 7.7 GPa and ~800 K in the form of nanoparticles isolated in the NaCl matrix. The phase transition rs-ZnO → w-ZnO in nanocrystalline zinc oxide under ambient pressure was experimentally studied for the first time by using differential scanning calorimetry and high-temperature X-ray diffraction analysis. It was shown that the transition occurs in the temperature range from 370 to 430 K and its enthalpy at 400 K is -10.2 ± 0.5 kJ mol^{-1}.

Key words: zinc oxide, high-pressure synthesis, phase transitions.

Hexagonal ($P6_3mc$) zinc oxide with the wurtzite structure, w-ZnO, is a direct-band semiconductor ($E_g = 3.4$ eV) with the highly ionic bond,[1] whereas cubic ($Fm3m$) zinc oxide with the rock salt structure, rs-ZnO, is an indirect semiconductor with the band gap energy $E_g \approx 2.7$ eV at 11 GPa.[2]

Under normal conditions, wurtzite ZnO is thermodynamically stable and at pressures about 9 GPa and room temperature is transformed into the cubic modification.[3] The reverse transition is observed[4,5] only upon the subsequent pressure drop to 2 GPa, indicating considerable hysteresis between the direct (w → rs) and reverse (rs → w) phase transitions in ZnO at room temperature. The hysteresis width decreases with the temperature increase, and above 1200 K the branches of the direct and reverse transition are brought together under a pressure about 6 GPa,[4,5] which can be considered as an equilibrium pressure of this phase transition. The cubic phase of zinc oxide is stable only under pressures above 2 GPa and cannot be quenched down to ambient pressure.[4,5]

It was experimentally shown[6—8] that for nanocrystalline w-ZnO the direct transition occurs under higher (>9 GPa) pressures and the samples with a particle size of ~12 nm treated at pressures higher than 15 GPa retain cubic structure after the pressure was released.[6,7] However, since all experiments mentioned were carried out in diamond anvils, it cannot be excluded that residual pressures are retained in the sample after pressure release.

The purpose of the present work is to study the possibility to stabilize cubic zinc oxide synthesized under relatively low (~7 GPa) pressures in the sodium chloride matrix.

Experimental

Sodium chloride (special-purity grade) and monodispersed nanoparticles of wurtzite zinc oxide with the average size ~50 nm, synthesized by the thermal decomposition of zinc acetate in diethylene glycol by the earlier described method,[9] were used for the preparation of the starting mixtures. A mixture of w-ZnO and NaCl nanoparticles was ground in an agate mortar and then compacted in a steel press mold under a pressure of 1250 bar.

Cubic ZnO was synthesized in a high-pressure apparatus of the toroid type[10] under a pressure of 7.7 GPa in the temperature interval from 700 to 900 K. For the pressure calibration of the cell, the phase transition Bi_{III-V} (7.7 GPa, room temperature) was used, whereas the Pt10%Rh—Pt thermocouples were used for the temperature calibration ignoring the pressure effect on the thermal emf. Gold capsules were used to insulate the samples from the high-pressure assembly. The samples were loaded at room temperature, and then the temperature was raised to the required value. After the isothermal heating for 15 min, the samples were quenched by switching off the power and slowly decompressed down to ambient pressure.

X-ray diffraction study of the synthesized samples and precision determination of the lattice parameters were performed on

Published in Russian in *Izvestiya Akademii Nauk. Seriya Khimicheskaya,* No. 2, pp. 318—321, February, 2010.
1066-5285/10/5902-0325

a TEXT 3000 INEL (λ = 1.54056 Å) diffractometer. A sample of LaB_6 (a = 4.15695 Å) was used as standard for detector adjustment. Lattice parameters were determined by the full-profile analysis with allowance for corrections to X-ray absorption and the shift of the sample surface from the diffraction plane. The size of ZnO crystallites was determined by the Debye—Scherrer equation taking into account the instrumental function.

The quenched samples were studied *in situ* at temperatures below 1000 K *in vacuo* by X-ray diffractometry on a Rigaku D/MAX 2500 diffractometer ($CuK\alpha_{1,2}$ radiation) in the angle scanning range 30—65° (2θ) using an HT-1500 high-temperature attachment. The 2θ scan rate was 5 deg min^{-1} at a linear heating rate of 2 deg min^{-1}, which corresponded to the change in the temperature of the sample by 15 K during detection of each diffraction pattern.

The thermoanalytical study of the quenched samples in the temperature range from 300 to 900 K was carried out by differential scanning calorimetry (DSC) on a NETZSCH DSC 204 F1 calorimeter in the regime of continuous heating with rates 2, 5, and 10 deg min^{-1} in high-purity (>99.998%) argon. Aluminum ampules were used as holders of the sample. The calorimeter was calibrated by using the phase transitions of the standard substances (Hg, KNO_3, In, Sn, Bi, and CsCl with purity not lower than 99.99%). The experimental data were processed using the NETZSCH Proteus Analysis program package.

Results and Discussion

At 7.7 GPa and temperatures below 1000 K a pristine w-ZnO nanopowder was used as a starting material, the quenching resulted in the formation of a mixture of rs-ZnO and w-ZnO in various ratios rather than the single phase cubic zinc oxide. Therefore, all further experiments were carried out only with w-ZnO in the NaCl matrix.

Cubic ZnO was synthesized at 700—900 K, which allowed us to ensure the completeness of the w-ZnO → rs-ZnO phase transition at 7.7 GPa and to avoid an increase in the ZnO nanoparticle size at higher temperatures.

According to the X-ray diffraction data of the quenched samples, the complete stabilization of the cubic structure of the zinc oxide nanoparticles in the sodium chloride matrix is observed only starting from the ratio ZnO/NaCl = = 1 : 3 (Table 1). The diffraction pattern of the salt rs-ZnO/NaCl nanocomposite (1 : 3) with the maximum content of zinc oxide (25 wt. %) is presented in Fig. 1. All reflections in the diffraction patterns are assigned either to rs-ZnO (JCPDS No. 77-0191; Fm3m, a = 4.28 Å) or to NaCl (JCPDS No. 05-0628; Fm3m, a = 5.642 Å); no reflections of other phases, including w-ZnO, are observed. The average size range of coherent scattering areas of rs-ZnO, estimated from the reflection broadenings in the diffraction patterns from the Debye—Scherrer equation, is almost the same for all salt composites listed in Table 1, being ~50 nm. This indicates that the size range of the ZnO nanoparticles does not change during the phase transition under the conditions of high pressures and temperatures.

When the initial mixture w-ZnO/NaCl contains more than 33 wt. % zinc oxide, the quenched samples represent a mixture of rs-ZnO and w-ZnO, *i.e.*, only the partial stabilization of the cubic structure of zinc oxide in the salt nanocomposites is observed after quenching. If micropowders of w-ZnO (99.99%, Aldrich, 325 mesh) with an average particle size of ~44 μm are used as the starting material, the cubic ZnO phase is not quenched at none of the w-ZnO/NaCl ratios in the starting mixtures. This indicates that the starting zinc oxide has some critical particle size, above which no stabilization of rs-ZnO can be achieved in the salt nanocomposites under normal conditions.

In a special series of experiments we have shown that the dissolution of the salt matrix of the rs-ZnO/NaCl nanocomposites in distilled water initiates the reverse phase transition rs-ZnO → w-ZnO, and after the complete removal of NaCl the sample represents w-ZnO with trace amounts of rs-ZnO. From the results obtained a conclusion can be made that the salt matrix plays the key role in the stabilization of the rs-ZnO nanoparticles synthesized at high pressures and temperatures after their quenching.

At room temperature the rs-ZnO nanoparticles in the sodium chloride matrix exhibit no tendency to the transition to w-ZnO for at least 5—6 months. For a longer

Table 1. Results of the thermoanalytical study of the salt nanocomposites rs-ZnO/NaCl

ZnO : NaCl[a]	Q[b]/kJ mol^{-1}	T_{max}/K at v_T[c]		
		2	5	10
1 : 5	−10.2±0.4	384	392	399
1 : 4	−10.9±0.4	387	—	404
1 : 3	−9.8±0.4	390	399	406

[a] Weight ratio.
[b] Q is the heat effect.
[c] T_{max} is the temperature of the phase transition maximum at different heating rates, v_T/deg min^{-1}.

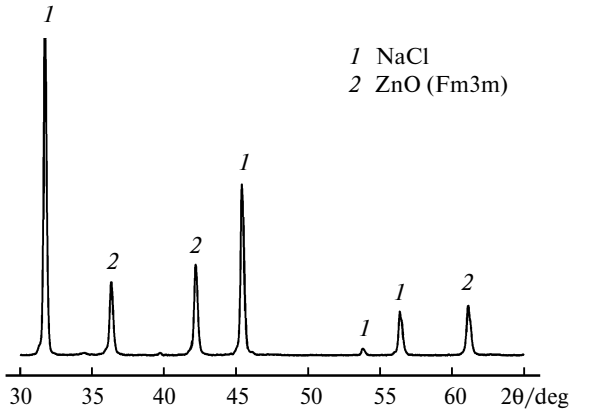

Fig. 1. Diffraction pattern of the nanocomposite rs-ZnO/NaCl (1 : 3) synthesized at 7.7 GPa and 800 K.

storage period (1 year), the partial reverse transition rs-ZnO → w-ZnO is observed in the samples and finally, after two years, the nanoparticles of cubic zinc oxide are completely transformed into wurtzite zinc oxide. Thus, it can be asserted that at room temperature the salt matrix kinetically impedes the reverse phase transition of zinc oxide from the metastable cubic modification to thermodynamically equilibrated wurtzite.

Thermal stability of the as-synthesized rs-ZnO/NaCl nanocomposites of different composition (see Table 1) under atmospheric pressure was studied *in situ* by X-ray diffraction analysis and differential scanning calorimetry. The diffraction patterns of the salt nanocomposite with rs-ZnO/NaCl = 1 : 3 obtained *in situ* are presented in Fig. 2. It can be seen in the left part of Fig. 2 that the reflection (002) of w-ZnO appears at 365 K and its intensity increases during further temperature rise. The right part of Fig. 2 shows the corresponding decrease in the intensity of the reflection (200) of rs-ZnO, which disappears completely at 425 K. Thus, two phases of zinc oxide in the NaCl matrix coexist in the temperature range 365—425 K.

Figure 3 shows the temperature dependence of the integral intensity reflection (200) of rs-ZnO normalized to the corresponding 300 K value. The curve has the classical S-shaped pattern, *i.e.*, at low temperature the transition rate is low, then it increases sharply with temperature, passes through a maximum at ~384 K, and further decreases to zero at temperatures above 430 K.

Upon further heating of the nanocomposites in the temperature range from 430 to 970 K the intensities of w-ZnO reflection increase noticeably, most likely, due to an increase in the degree of crystallinity of this phase. However, according to the DSC data, this process is not accompanied by any heat effect.

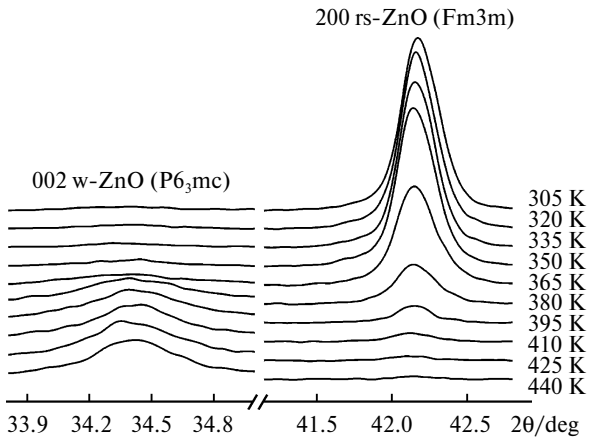

Fig. 2. Regions of the diffraction patterns of the nanocomposite rs-ZnO/NaCl (1 : 3) obtained by *in situ* linear heating with a rate of 2 deg min^{-1}. The reflections (200) of rs-ZnO and (002) of w-ZnO were chosen as the most intense non-overlapping reflections of the phases studied.

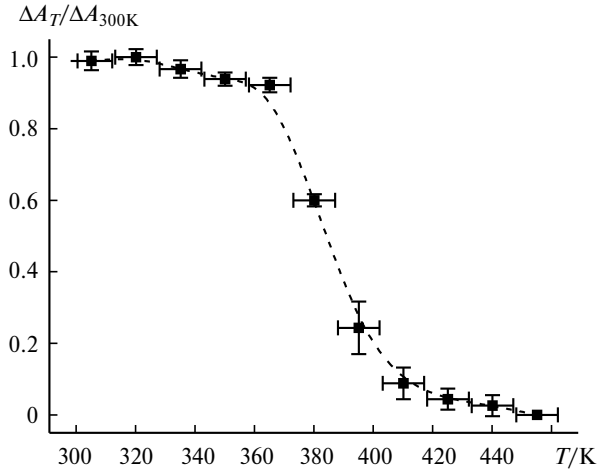

Fig. 3. Temperature dependence of the ratio of the integral surface area of the reflection (200) of rs-ZnO to the surface area of this reflection at 300 K.

The results of the thermoanalytical study of the 1 : 3 and 1 : 5 salt nanocomposites are presented in Fig. 4 and Table 1. At temperatures higher than 380—430 K, the DSC curves contain the pronounced exothermic effect, which can unambiguously ascribed to the irreversible structural transition of cubic zinc oxide to the wurtzite phase, which is well consistent with the results of high-temperature *in situ* X-ray diffraction analysis. As can be seen from Table 1, for all rs-ZnO/NaCl ratios studied the increase in the heating rate is accompanied by an increase in the peak temperature.

Along with the main exothermic effect, the thermoanalytical curve of the nanocomposite with the maximum content of rs-ZnO (1 : 3) shows the weak exothermic effect at 350—370 K (see Fig. 4, *b*), which can be attributed to the phase transition of submicronic aggregates of the rs-ZnO nanoparticles. It can be assumed that the transition rs-ZnO → w-ZnO in similar aggregates occurs at lower temperatures than in the case of the rs-ZnO nanoparticles isolated in the salt matric. For a more "dilute" composition with rs-ZnO/NaCl = 1 : 4 , this effect is less pronounced and is absent at all for the composition with rs-ZnO/NaCl = 1 : 5 (see Fig. 4, *a*). No other processes accompanied by the heat evolution or absorption were observed in the whole temperature range studied (up to 870 K). Thus, based on the data of DSC and high-temperature differential scanning calorimetry, we can conclude that the structural transition Fm3m → P6$_3$mc observed for zinc oxide in the sodium chloride matrix at ambient pressure is the monotropic first-order phase transition[11] that occurs without formation of any intermediate phases.

For the 1 : 3 and 1 : 4 rs-ZnO/NaCl nanocomposites, the heat effect of the phase transition at a given heating rate was determined as the sum of two observed exothermic effects taking place at 350—370 K and 380—430 K, respectively. The thermal effect values obtained at differ-

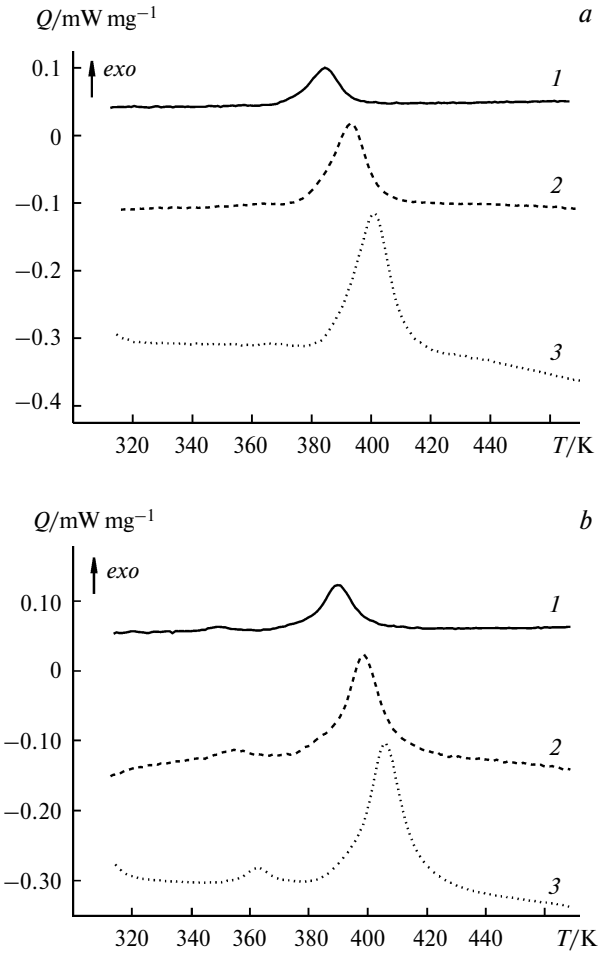

Fig. 4. DSC curves of the salt nanocomposites rs-ZnO/NaCl of the composition 1 : 5 (*a*) and 1 : 3 (*b*) detected at the heating rate 2 (*1*), 5 (*2*), and 10 deg min^{-1} (*3*) (*Q* is the specific heat flow).

ent heating rates were averaged for each composition (see Table 1). The enthalpy of phase transition at 400 K was determined by averaging over all experimental values of heat effects and is equal to -10.2 ± 0.5 kJ mol^{-1}.

The enthalpy of the reverse rs-ZnO → w-ZnO phase transition determined in this work differs by the order of magnitude from both the enthalpy values of the direct w-ZnO → → rs-ZnO phase transition estimated from the data on solubility in borate melts ($\Delta_{tr}H^\circ_{297\ K} = 24.5\pm3.6$ kJ mol^{-1})[12,13] and temperature dependences of the emf of the electrochemical cells with the ZnO-based electrodes ($\Delta_{tr}H^\circ_{1173\ K} =$ $= 17.4\pm1.3$ kJ mol^{-1}),[14] and the value $\Delta_{tr}H^\circ_{297\ K} =$ $= 3.3$ kJ mol^{-1},[3] calculated by the Clapeyron—Clasius equation from the experimental data on the synthesis of rs-ZnO at high pressures. Unlike the direct calorimetric determination of the enthalpy of the rs-ZnO → w-ZnO phase transition, performed in the present work, the enthalpy vlaues reported earlier[3,12—14] were obtained from indirect thermodynamic data and, hence, should be considered as estimates.

Thus, in the present work we have shown for the first time that the cubic phase of zinc oxide can be synthesized in the form of salt nanocomposites, which are kinetically stable under ambient pressure up to temperatures of about 370 K. This provides new possibilities for studying the physical and chemical properties of cubic ZnO. According to the DSC data, at ambient pressure the rs-ZnO → → w-ZnO phase transition in the salt nanocomposites occurs in the 370—430 K range and its enthalpy at 400 K is -10.2 ± 0.5 kJ mol^{-1}.

We thank O. O. Kurakevich for help in high-pressure experiments and to V. A. Mukhanov for valuable comments. P. S. Sokolov is grateful to the French Government for financial support (Bourse de co-tutelle No. 1572-2007).

This work was financially supported by the Russian Foundation for Basic Research (Project No. 09-03-90442-Ukr_f_a).

References

1. C. Klingshirn, *Phys. Status Solidi B*, 2007, **244**, 3027.
2. J. A. Sans, A. Segura, F. J. Manjon, B. Mari, A. Munoz, *Microelectron. J.*, 2005, **36**, 928.
3. C. H. Bates, W. B. White, R. Roy, *Science,* 1962, **137**, 993.
4. K. Kusaba, K. Syono, T. Kikegawa, *Proc. Jpn Acad. Ser. B*, 1999, **75**, 1.
5. F. Decremps, J. Zhang, R. C. Liebermann, *Europhys. Lett.*, 2000, **51**, 268.
6. J. Z. Jiang, J. S. Olsen, L. Gerward, D. Frost, D. Rubie, J. Peyronneau, *Europhys. Lett.*, 2000, **50**, 48.
7. F. Decremps, J. Pellicer-Porres, F. Datchi, J. P. Itie, A. Polian, F. Baudelet, J. Z. Jiang, *Appl. Phys. Lett.,* 2002, **81**, 4820.
8. E. Grzanka, S. Gierlotka, S. Stelmakh, B. Palosz, T. Strachowski, A. Swiderska-Srode, G. Kalisz, W. Lojkowski, F. Porsch, *Z. Kristallogr. Suppl.,* 2006, **23,** 337.
9. E. W. Seeling, A. Yamilov, H. Cao, R. P. H. Chang, *Mater. Chem. Phys.*, 2003, **80**, 257.
10. L. G. Khvostantsev, V. N. Slesarev, V. V. Brazhkin, *High Press. Res.*, 2004, **24**, 371.
11. J. B. Clarke, J. W. Hastie, L. H. E. Kihlborg, R. Metselaar, M.M. Thackeray, *Pure Appl. Chem.*, 1994, **66**, 577.
12. A. Navrotsky, A. Muan, *J. Inorg. Nucl. Chem.,* 1971, **33**, 35.
13. P. K. Davies, A. Navrotsky, *J. Solid State Chem.,* 1981, **38**, 264.
14. J. S. Kachhawaha, V. B. Tare, *Solid State Ionics*, 1981, **5**, 575.

Received March 24, 2009;
in revised form November 18, 2009